Am J Cancer Res 2023;13(2):485-497
www.ajcr.us /ISSN:2156-6976/ajcr0145916

Original Article

POM121 promotes the proliferation and metastasis of gastric cancer via PI3K/AKT/MYC pathway

Changyuan Kang[1], Lizhou Jia[2], Lei Hao[1], Ning Zhang[2], Yang Liu[2], Lingli Zhang[3]

[1]Basic Medical Sciences College, Inner Mongolia Medical University, Hohhot 010000, Inner Mongolia, China; [2]Central laboratory, Bayannur Hospital, Bayannur 015000, Inner Mongolia, China; [3]Department of Ophthalmology, Inner Mongolia Autonomous Region People's Hospital, Hohhot 010017, Inner Mongolia, China

Received August 14, 2022; Accepted January 7, 2023; Epub February 15, 2023; Published February 28, 2023

Abstract: Nuclear pore membrane protein 121 (POM121) is a part of the nuclear pore complex, which regulates intracellular signaling and maintains normal cellular functions. However, the role of POM121 in gastric cancer (GC) remains unclear. Quantitative real-time polymerase chain reaction was performed to detect POM121 mRNA in 36 pairs of GC and adjacent non-tumor tissues. POM121 protein expression was determined by immunohistochemistry in 648 GC tissues and 121 normal gastric tissues. Connections between POM121 levels, clinicopathological parameters, and the prognosis of GC patients were explored. The influence of POM121 on proliferation, migration, and invasion was detected in vitro and vivo. The mechanism underlying the involvement of POM121 in GC progression was demonstrated via bioinformatics analysis and Western blot. Both the mRNA and protein levels of POM121 in GC tissues were higher than those in normal gastric tissues. High POM121 expression in GC was associated with deep invasion, advanced distant metastases and TNM stage, and positive HER2 expression. A negative connection was found between POM121 expression and the overall survival (OS) of GC patients. Downregulation of POM121 inhibited the proliferation, clone formation, migration, and invasion of GC cells, and overexpression of POM121 showed the opposite trend. POM121 promoted the phosphorylation of PI3K/AKT pathway and increased the expression of MYC. In conclusion, this study suggested that POM121 has the potential to act as an independent prognostic factor for GC patients.

Keywords: POM121, gastric cancer, proliferation, metastasis, PI3K/AKT, MYC

Introduction

Gastric cancer (GC) is one of the most common and fatal cancers globally, with most of the new cases diagnosed in developing countries [1]. The prevalence of GC is second only to lung carcinoma and becomes the second leading cause of cancer-related mortality in China [2]. The symptoms of early-stage GC are not prominent, thus a large proportion of GC patients have advanced-stage disease at the time of diagnosis. Despite the continuous advances in GC treatment methods, the prognosis of most GC patients is still not optimistic. Therefore, the identification of new prognostic biomarkers and therapeutic strategies is indispensable to curing this disease and improving quality of life for GC patients.

The nuclear pore complex (NPC) is the sole gateway embedded in the nuclear envelope and controls transport between the cytoplasm and the nucleus [3]. NPC is reported to have many transport-independent functions such as chromatin organization [4], RNA processing [5], DNA repair [6], transcriptional regulation [7], and cell cycle control [8]. NPC plays an important role in maintaining the homeostasis of cellular signaling and protein localization, the dysregulation of which is closely related to carcinogenesis [9]. The involvement of several nucleoporins (NUPs) has been demonstrated in tumorigenesis and progression. TPR is the first validated NUP associated with cancer in osteogenic sarcoma cells and is thought to be involved in the early stages of gastric carcinomas [10]. NUP98 fusion proteins are important in many myeloid malignancies, and NUP98 acts as a potential tumor suppressor by regulating the expression of genes targeted by p53 [11-13]. NUP62, NUP88, NUP214, and NUP358/RANBP2 are also connected with tumorigene-

sis [14]. POM121 is reported to promote lethal prostate cancer, but little is known about its role in GC [15].

The present study aimed to determine the role of POM121 in GC. The differences in POM121 expression in GC tissues and normal tissues were investigated. We also analyzed the relationships between the POM121 level and clinicopathological features of GC patients. Then the POM121 expression was downregulated, and the biological behavior of GC cells was detected. Finally, the variation of the PI3K/AKT/MYC pathway was demonstrated in the mechanisms of POM121 in GC progression. Our findings indicate that POM121 may be a potential prognostic biomarker and new therapeutic target for GC patients in the future.

Materials and methods

POM121 expression in database

The gene expressions of GC patients have downloaded from The Cancer Genome Atlas (TCGA) Data Portal website (https://portal.gdc.cancer.gov/projects/TCGA-STAD), including 27 GC tissues and 27 normal gastric tissues. The data were analyzed by R package ggplot2.

Human gastric tissue samples

All pathological specimens were collected from the Pathology Department of Inner Mongolia Autonomous Region People's Hospital between February 2004 and November 2014. A total of 983 tissue samples were obtained from patients after surgery or gastric endoscopic biopsy, including 684 GC tissues, 121 paired para-carcinoma tissues, 37 chronic gastritis, 34 intestinal metaplasia, 46 low-grade intraepithelial neoplasia, and 61 high-grade intraepithelial neoplasia. None of the volunteers underwent any chemotherapy or radiotherapy before surgery or biopsy. Histopathological confirmation of tissues was performed by two pathologists blinded to each other. Clinicopathological data such as age, tumor size, grade, lymph node status, and TNM stage were retrieved from patient medical records. This study was performed following medical ethical standards and was approved by the Ethics Committee of Inner Mongolia Medical University. Written informed consent were obtained from all study participants.

Quantitative real-time polymerase chain reaction (qRT-PCR)

A total of 36 GC tissues and 36 normal tissues were prepared to detect POM121 mRNA expression. Total RNA was extracted from frozen tissues using TRIzol Plus RNA Purification Kit (#12183555, Invitrogen, USA) following the manufacturer's instructions. Reverse transcription was performed with SuperScript First-Strand Synthesis System for RT-PCR (#11904018, Invitrogen). Amplification of the cDNA with the Power SYBR Green PCR Master Mix (#4368706, Applied Biosystems, USA) was performed using a StepOne Real-Time PCR System (Applied Biosystems). The human POM121 primers used were as follows: forward 5'-AGTGGCAGTGGACATTCAGC-3', and reverse 5'-CGTAAGC GCCTGTCAAGGA-3'. The human *GAPDH* primers were as follows: forward 5'-CTGGGCTACACTGAGCACC-3', and reverse 5'-AAGTGGTCGTTGAGGGCAA TG-3'. GAPDH was utilized to normalize POM121 gene expression, and $2^{-\Delta\Delta Ct}$ was calculated as the level of POM121. All analyses were performed independently three times.

Tissue microarray (TMA) construction and immunohistochemistry (IHC)

All tissue samples were embedded in paraffin after 4% formalin fixation. A TMA was constructed with paraffin-embedded blocks of donor tissues using a Quick Ray Master UATM-272A (UNITMA, Korea). Cores biopsies of 3 mm in diameter were acquired from donor blocks, and then were cut into 3 μm thicknesses. Sections of the tissue blocks were placed on glass slides and deparaffinized in gradient ethanol. TMA was heated in citrate buffer (0.01 M, pH 6.0) for antigen retrieval, and then incubated with 3% H_2O_2 to block endogenous peroxidase activity. Sections were incubated with a rabbit anti-POM121 polyclonal primary antibody (#ab190015, Abcam, UK) and were stained using the Lab Vision Ultra Vision ONE Detection System (Invitrogen, USA). The score of staining intensity was categorized into four levels: 0 (negative), 1 (weakly positive), 2 (moderately positive), and 3 (strongly positive). The final score was set as 100 × the product of the staining intensity and the percentage of cells stained. Immunohistochemical staining for POM121 was estimated by two pathologists blinded to patient information. The cutoff value

was selected as 115 by the X-tile-based TMA data analysis. Scores between 0 and 115 represented a low expression of POM121, and scores between 116 and 300 represented a high expression of POM121.

Stable cell lines

Human GC cell lines BGC823, MG803, SGC-7901, and HGC27 (FuHeng Biology, Shanghai, China) were cultured in an incubator with 5% CO_2 at 37°C. The lentiviral-based shRNA targeting POM121 and lentiviral vector were purchased from Genechem Co., Ltd., Shanghai, China. The two cells were infected with the lentivirus expressing shNC or shPOM21, respectively. Lentivirus-mediated POM121-cDNA and empty vector were transfected into SGC7901 and HGC27 cells, which were called NC and ovPOM121.

Western blot

Total protein was extracted from different stable cells using RIPA buffer (#89901, Thermo Scientific, USA). The protein samples were mixed with loading buffer (#P0015A, Beyotime, China) and then degenerated at 100°C for 10 min. The same amounts of proteins were separated by sodium-dodecyl-sulfate-polyacrylamide gel electrophoresis and transferred to a polyvinylidene fluoride membrane. The membrane was incubated with the primary antibodies to POM121 (#83525, CST, USA), P-PI3K (#17366, CST), PI3K (#4249, CST), P-AKT (#ab38449, Abcam, USA), AKT (#ab8805, Abcam), MYC (#ab9106, Abcam), and GAPDH (#AM4300, Invitrogen) at 4°C overnight. After three rinses with PBST buffer for 15 min each time, the membrane was incubated with horseradish-peroxidase-labeled secondary antibodies for 2 h at room temperature. Then, the membrane was rinsed with PBST and developed with Highsig ECL Western Blotting Substrate (#180-5001, Tanon, China).

CCK-8 assay

The cells of each group were planted in a 96-well plate with 5×10^3 cells/well. The cell proliferation level was detected at 24 h, 48 h, 72 h, and 96 h, respectively. The cells in each well were incubated with a 100 μl mixture of RPMI 1640 medium and CCK-8 reagent (9:1) at 37°C in darkness for 2 h. The absorbance of each well in OD450 was measured with a microplate reader.

Clone formation assay

The cells of each group were planted in a 6-well plate with 600 cells/well. The plate was cultured in an incubator with 5% CO_2 at 37°C for 2 w. Then the cells were rinsed with PBS buffer three times gently and soaked in methanol for 30 min. The cells were incubated with 0.5% crystal violet solution at room temperature for 30 min. Finally, the cell clones were rinsed by ddH_2O.

Transwell assays

Migration assay: The cells were suspended in a serum-free medium and planted in the upper chamber. Place the Transwell chamber into the 24-well plate which contains medium with 20% FBS. The cells were cultured in an incubator for 24 h. The cells in the upper chamber were gently wiped with a swab. The chamber was fixated with 4% paraformaldehyde for 30 min and then stained with 0.2% crystal violet for 30 min. After rinsing and drying, cell clones were observed and counted.

Invasion assay: Matrigel basement membrane matrix (#356234, BD Biosciences, USA) was diluted with serum-free RPMI 1640 medium at a ratio of 1:3 at 4°C. 100 μl Matrigel mixture was spread on the surface of the upper chamber and dried at 37°C for 1 h. The following steps were the same as those of the migration assay.

Subcutaneous tumor model

A total of 12 five-week-old male BALB/C nude immunodeficient mice were purchased from Vital River Laboratory Animal Technology Co., Ltd. (Shanghai, China). Cells of the BGC823 group were suspended with a density of 1×10^7/ml. Cell suspensions (100 μl) were injected into the left upper extremity armpit, and tumor size was measured with a vernier caliper every 6 days. The tumor volume was calculated as longest diameter × shortest diameter^2/2.

Protein-protein interactions (PPI) and correlation analysis

To explore the possible mechanism of POM121, a putative protein–protein interaction network around POM121 was explored by STRING v11.5 (https://cn.string-db.org/). The visualization of PPI was performed in Cytoscape v3.9.1. The correlation between POM121 and MYC was cal-

culated to use the Xiantao website (https://www.xiantao.love/) based on the RNAseq data of 375 GC patients downloaded from the TCGA database.

Statistical analysis

All statistical analyses were conducted on SPSS 19.0 statistical software package (SPSS, Inc., USA). The difference between the two groups was analyzed by paired test-test if the data came in pairs. If not, independent T test. Student's *t*-test was used to compare differences in POM121 expression between GC and non-tumor tissues. The associations between the clinical characteristics of patients and POM121 expression were evaluated by the Chi-square test or Trend test. The Kaplan-Meier method was used to calculate overall survival, and the log-rank test was performed to analyze survival curves. Statistical significance was set at $P<0.05$.

Results

POM121 expression in GC tissues

The data of the TCGA database demonstrated that the gene expressions of POM121 in GC tissues were significantly higher than these in normal gastric tissues (P<0.001, **Figure 1A**). POM121 mRNA expression in 36 pairs of GC tissues and peritumoral normal tissues was examined, and the result confirmed that POM121 mRNA expression in GC tissues was significantly higher than that in matched normal gastric tissues ($P<0.001$, **Figure 1B**).

To confirm the protein expression of POM121 in gastric tissues, we performed IHC analysis on TMAs consisting of 684 GC tissues, 121 adjacent non-tumor tissues, 37 chronic gastritis, 34 intestinal metaplasia, 46 low-grade intraepithelial neoplasia, and 61 high-grade intraepithelial neoplasia. IHC staining demonstrated that POM121 was mainly expressed in the nuclear envelope (**Figure 1D**). Our results showed only 12.4% (15/121) of normal gastric tissues presented high POM121 expression, while the occurrence rate of high POM121 expression was 63.0% (433/684) in GC tissues. High POM121 expression was also detected more often in chronic gastritis (24.32%, 9/37), low-grade intraepithelial neoplasia (26.09%, 12/46), and high-grade intraepithelial neoplasia (22.95%, 14/61) than in neighboring tumor tissues (**Figure 1C**).

Association between POM121 expression and clinicopathological characteristics

To ascertain if POM121 affects the clinical manifestations of GC patients, we analyzed the association between POM121 expression and pathological features. POM121 level was significantly linked to depth of invasion (χ^2 = 17.831, P = 0.001), distant metastases (χ^2 = 7.505, P = 0.006), TNM stage (χ^2 = 18.412, P = 0.001), and HER2 expression (χ^2 = 6.285, P = 0.012). However, POM121 expression was found to have no connection with sex, age, histological type, differentiation, lymph node metastases, preoperative CEA, preoperative CA199, and *Helicobacter pylori*. Our results indicated that gastric carcinomas with high POM121 expression tend to enter a more advanced clinical stage with distant metastases than those with low POM121 expression (**Table 1**).

Relationship between POM121 expression and prognosis for GC patients

The median survival time of the 684 patients we investigated was 27±5.78 months. Patients with high POM121 expression showed significantly shorter median survival time than patients with low POM121 expression (21±2.43 vs 36±5.69 months, $P<0.001$; **Figure 2A**). Distant metastases and TNM stages were also significantly connected with OS (**Figure 2**). Univariate analysis indicated that risk factors for OS of GC patients included POM121 expression ($P<0.001$), age (P = 0.008), differentiation ($P<0.001$), distant metastasis ($P<0.001$), TNM stage ($P<0.001$), and HER2 expression ($P<0.001$). Multivariate analysis suggested that high POM121 expression (HR, 1.502; 95% CI: 1.197-1.883; $P<0.001$) was significantly associated with poor OS, as well as differentiation (HR, 1.137; 95% CI: 1.006-1.287; P = 0.040), distant metastasis (HR, 2.539; 95% CI: 1.967-3.277; $P<0.001$), TNM stage (HR, 1.180; 95% CI: 1.089-1.279; $P<0.001$), and HER2 expression (HR, 0.329; 95% CI: 0.287-0.377; $P<0.001$) (**Table 2**). These results showed that POM121 may be an independent prognostic biomarker for GC patients.

Decreased POM121 expression hindered the progression of GC

To explore the effect of POM121 on GC development, POM121 expression was knockdown in GC cell lines BGC823 and MGC803 (**Figure 3A**). CCK-8 assay showed that POM121 down-

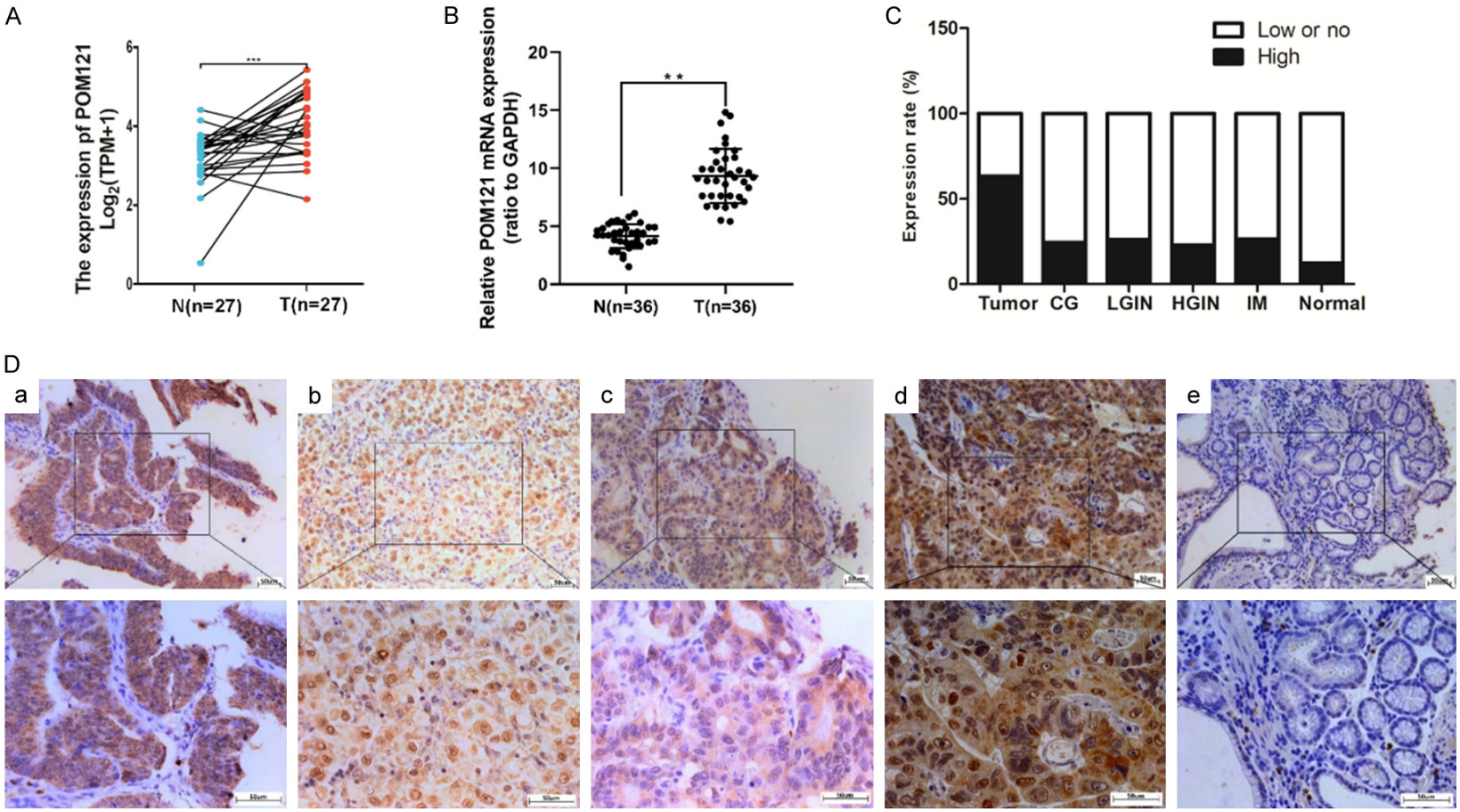

Figure 1. POM121 expression in gastric tissues. A: POM121 expression in GC tissues and normal tissues in TCGA database. B: POM121 mRNA expression in 36 pairs of GC tissues and peritumoral normal tissues. C: POM121 protein expressions in gastric tissues. D: Representative images of POM121 protein in gastric tissues. a. Gastric papillary adenocarcinoma with high POM121 expression (staining score = 280). b. Low-differentiated adenocarcinoma with high POM121 expression (staining score = 260). c. Moderate-differentiated adenocarcinoma with low POM121 expression (staining score = 220). d. Well-differentiated adenocarcinoma with low POM121 expression (staining score = 190). e. Pericarcinomatous tissues with no POM121 expression (staining score = 0). (Original views ×4, bar = 500 μm; enlarged views ×40, bar = 50 μm). $^{**}P<0.01$, $^{***}P<0.001$.

Table 1. POM121 protein expression level and GC patient clinicopathological characteristics

Characteristics	n	POM121 expression (%)		Pearson χ^2	*P*-value
		Low or no	High		
Total	684	251	433		
Gender				2.928	0.087
Male	495	172 (34.75)	323 (65.25)		
Female	189	79 (41.80)	110 (58.20)		
Age				0.443	0.506
<60	256	98 (38.28)	158 (61.72)		
≥60	428	153 (35.75)	275 (64.25)		
Histological type				0.287	0.991
Tubular	485	180 (37.11)	305 (62.89)		
Mucinous	89	32 (35.96)	57 (64.04)		
Mixed (tubular and mucinous)	16	5 (31.25)	11 (68.75)		
Signet ring cell	45	16 (35.56)	29 (64.40)		
Others[a]	49	18 (36.73)	31 (63.27)		
Differentiation				1.281	0.527
Well	198	77 (38.89)	121 (61.11)		
Moderate	261	89 (34.10)	172 (65.90)		
Poor	225	85 (37.78)	140 (62.22)		
Depth of invasion				17.831	0.001*
Tis	23	14 (60.87)	9 (39.13)		
T1	78	36 (46.15)	42 (53.85)		
T2	138	57 (41.30)	81 (58.70)		
T3	405	137 (33.83)	268 (66.17)		
T4	40	7 (17.50)	33 (82.50)		
Lymph node metastasis				5.826	0.120
N0	258	93 (36.05)	165 (63.95)		
N1	193	72 (37.31)	121 (62.69)		
N2	117	52 (44.44)	65 (55.56)		
N3	116	34 (29.31)	82 (70.69)		
Distant metastasis				7.505	0.006*
M0	573	223 (38.92)	350 (61.08)		
M1	111	28 (25.23)	83 (74.77)		
TNM stage				18.412	0.001*
0	29	16 (55.17)	13 (44.83)		
I	110	49 (44.55)	61 (55.45)		
II	297	111 (37.37)	186 (62.63)		
III	183	64 (34.97)	119 (65.03)		
IV	65	11 (16.92)	54 (83.08)		
Preoperative CEA, ng/ml				4.347	0.114
<5	272	87 (31.99)	185 (68.01)		
≥5	373	149 (39.95)	224 (60.05)		
Unknown[b]	39	15 (38.46)	24 (61.54)		
Preoperative CA199, ng/ml				5.007	0.082
<37	246	96 (39.02)	150 (60.98)		
≥37	301	116 (38.54)	185 (61.46)		
Unknown[b]	137	39 (28.47)	98 (71.53)		

Helicobacter pylori				0.451	0.502
Positive	420	150 (35.71)	270 (64.29)		
Negative	264	101 (38.26)	163 (61.74)		
Her-2				6.285	0.012*
Negative	561	218 (38.83)	343 (61.14)		
Positive	123	33 (26.83)	90 (73.17)		

a: others include: papillary adenocarcinoma 12 cases; adeno-squamous carcinoma 10 cases; squamous cell carcinoma 9 cases; undifferentiated carcinoma 8 cases; neuroendocrine carcinoma 10 cases. b: Two unknown groups had no exact records, and thus, were not used in the *P*-value calculation. *$P<0.05$.

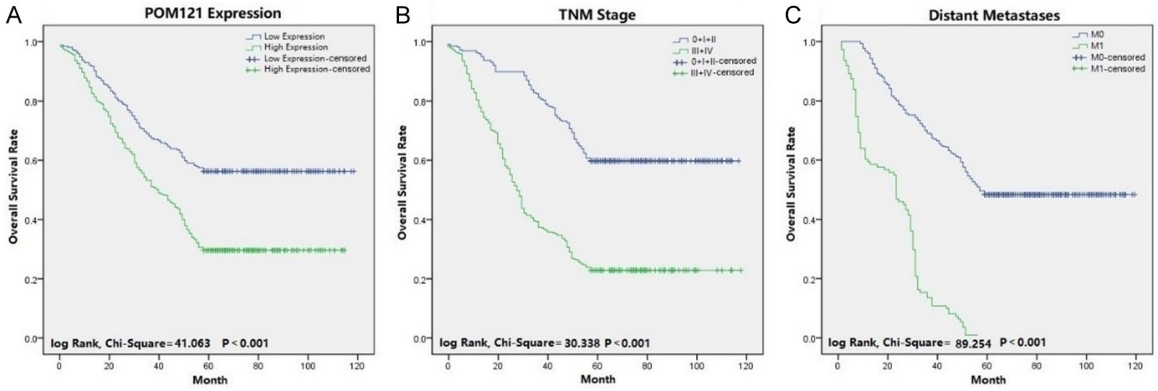

Figure 2. Survival curves of GC patients using the Kaplan-Meier method and the log-rank test. A: Overall survival curves for patients with low POM121 expression (blue line) and patients with high POM121 expression (green line). B: Overall survival curves by TNM stage, TNM 0, I and II (blue line), TNM III and IV (green line). C: Overall survival curves by distant metastases, M0 (blue line), M1 (green line).

Table 2. Univariate and multivariate analyses of the prognostic factors for overall survival in GC

	Univariate analysis			Multivariate analysis		
	HR	*P*-value	95% CI	HR	*P*-value	95% CI
POM121 expression						
High vs Low or no	2.020	<0.001*	1.619 2.520	1.502	<0.001*	1.197 1.883
Age (year)						
<60 vs ≥60	1.319	<0.001*	1.073 1.621	1.171	0.143	0.948 1.447
Gender						
Male vs Female	1.024	0.831	0.825 1.270			
Differentiation						
Well vs Moderate vs Poor	1.259	<0.001*	1.108 1.430	1.137	0.040*	1.006 1.287
Tumor disameter						
Tis + T1 + T2 vs T3 + T4	1.074	0.226	0.957 1.205			
Lymph node metastasis						
N0 vs N1 + N2	0.975	0.577	0.893 1.065			
Distant metastasis						
M0 vs M1	5.253	<0.001*	4.164 6.627	2.539	<0.001*	1.967 3.277
TNM stage						
0 + I + II vs III + IV	1.477	<0.001*	1.376 1.586	1.180	<0.001*	1.089 1.279
Her-2						
Negative vs Positive	0.270	<0.001*	0.238 0.306	0.329	<0.001*	0.287 0.377

HR: Hazard Ratio; CI: Confidence Interval. *$P<0.05$.

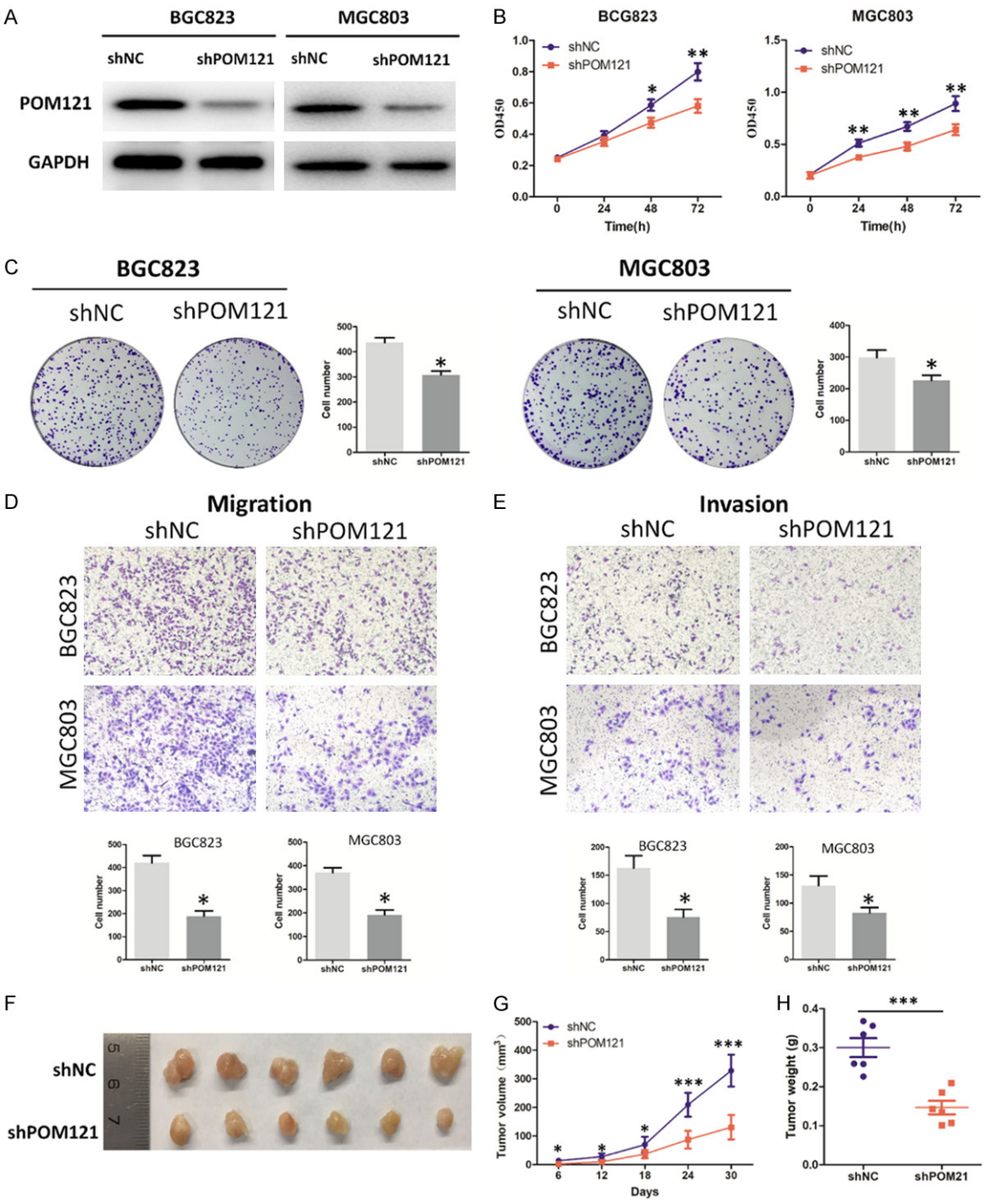

Figure 3. POM121 plays an oncogenic role in GC cells. A: POM121 expression of BGC823 and MGC803 cells after shPOM121 transfection. B: The proliferation of GC cells after POM121 knockdown. C: The clone formation of GC cells after POM121 silence. D: The migration of GC cells after downregulation of POM121. E: The invasion of GC cells after downregulation of POM121. F: The volumes of tumors in the xenograft mouse model. G: The growth curves of tumors in the xenograft mouse model. H: The weight of tumors in the xenograft mouse model.

regulation inhibited the proliferation of GC cells (**Figure 3B**). The result of the clone formation assay further confirmed the adverse impact of POM121 silence on cell viability (**Figure 3C**). Transwell assay demonstrated that the knockdown of POM121 hampered migration (**Figure 3D**) and invasion (**Figure 3E**) of GC cells. Finally, a tumor xenograft model was constructed to determine the influence of POM121 on GC development in vivo. The results displayed that

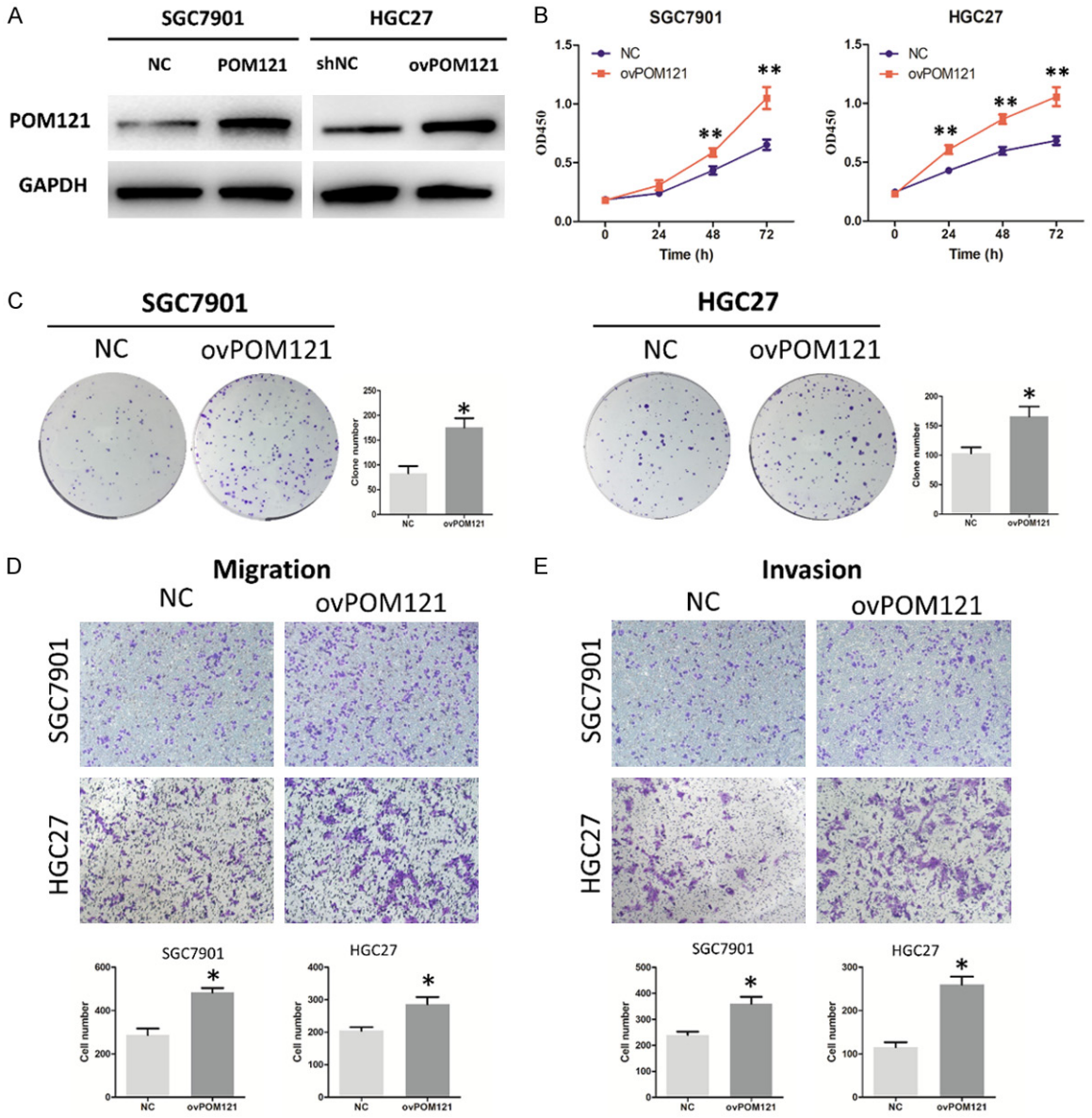

Figure 4. POM121 plays an oncogenic role in GC cells. A: POM121 expression of SGC7901 and HGC27 cells after ovPOM121 transfection. B: The proliferation of GC cells after POM121 overexpression. C: The clone formation of GC cells after POM121 overexpression. D: The migration of GC cells after upregulation of POM121. E: The invasion of GC cells after upregulation of POM121.

shPOM121 significantly decreased the volume and weight of the subcutaneous tumor (**Figure 3F-H**). These results suggested that the knockdown of POM121 restrained malignant biological properties in GC.

Overexpression of POM121 expression promoted the progression of GC

Furthermore, we overexpressed POM121 in GC cell lines SGC7901 and HGC27 (**Figure 4A**). CCK-8 assay showed that high POM121 expression promoted the proliferation of GC cells (**Figure 4B**). The clone formation assay confirmed the promoting impact of POM121 overexpression on cell viability (**Figure 4C**). Transwell assay demonstrated that increased POM121 level accelerated migration (**Figure 4D**) and invasion (**Figure 4E**) of GC cells. These results suggested that overexpression of POM121 expedited malignant biological properties in GC.

Silencing POM121 inhibited PI3K/AKT/MYC pathway

We constructed a protein interaction network to determine the putative mechanism as to

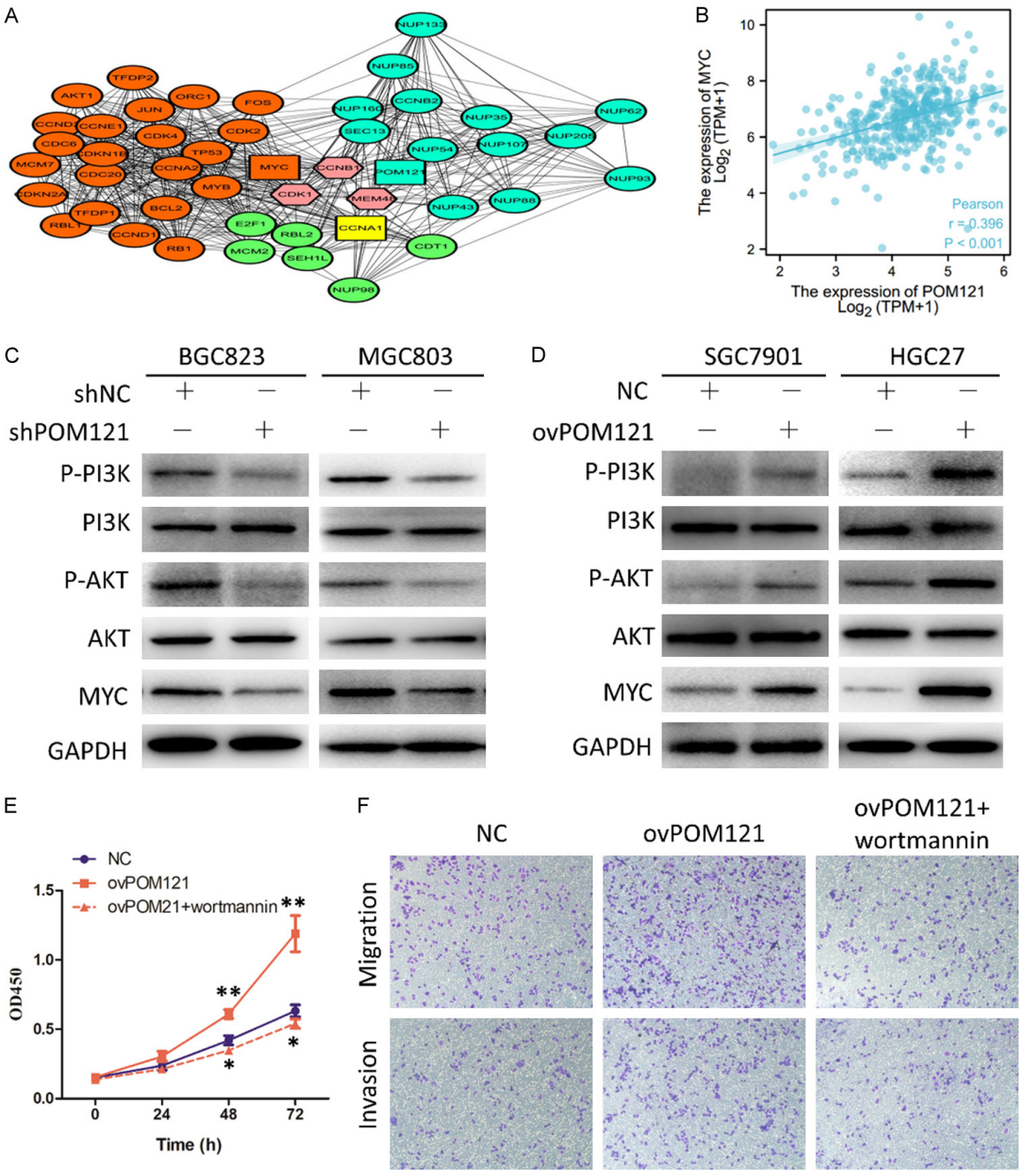

Figure 5. POM121 promotes GC progression through PI3K/AKT/MYC pathways. A: PPI network around POM121. B: Pearson correlation analysis between POM121 and MYC. C: Expression and phosphorylation of PI3K/AKT/MYC pathways in shPOM121 cells compared with the control. D: Expression and phosphorylation of PI3K/AKT/MYC pathways in ovPOM121 cells compared with the control. E: The proliferation of GC cells after wortmannin treatment. F: The migration and invasion of GC cells after wortmannin treatment.

how POM121 functions in GC. CCNB1, MYC, CDK1, and some other proteins were speculated to be linked to POM121 (**Figure 5A**). Pearson's correlation analysis revealed a positive correlation between POM121 and MYC (r = 0.396, *P*<0.001, **Figure 5B**). Western Blot also confirmed that silencing POM121 decreased the expression of MYC (**Figure 5C**). Furthermore, phosphorylation of the PI3K/AKT pathway was inhibited after the downregulation of POM121 (**Figure 5C**). Overexpression of POM-121 promoted the levels of MYC and phosphorylation of the PI3K/AKT pathway (**Figure 5D**). Furthermore, PI3K inhibitor wortmannin could

reverse the promoting effect of high POM121 expression on cell proliferation (**Figure 5E**), migration, and invasion (**Figure 5F**). The results described above approved that POM121 promoted GC progression via PI3K/AKT/MYC pathway.

Discussion

There are three transmembrane NUPs embedded in the mammalian nuclear membrane (POM121, NUP210, andNDC1), and POM121 is the least conserved and is only expressed in vertebrates [16, 17]. POM121 is essential in NPC and nuclear envelope assembly, empowering POM121 to have a vital role in nuclear transport [18]. Overexpression of POM121 has been detected in some tumors, including laryngeal cancer [19], colorectal cancer [20], oral squamous cell carcinoma [21], and lung cancer [22, 23]. In the present study, we investigated POM121 mRNA and protein expression. The qRT-PCR confirmed the overexpression of POM121 mRNA in gastric carcinoma, and GC tissues were more often detected with high POM121 protein expression (63.30%) than normal gastric tissues (12.40%). We also detected POM121 expression in chronic gastritis, intestinal metaplasia, and intraepithelial neoplasia, and found that less POM121 was expressed in abnormal gastric tissues than in GC tissues.

POM121 expression in GC tissues and the matched clinical information of 684 patients was analyzed. The results confirmed that GC patients with high POM121 levels were associated with deeper invasion, advanced distant metastases, TNM stage, and positive HER2 expression, suggesting POM121 expression may influence the progression, invasion, and metastases of GC. Except for differentiation, distant metastasis, TNM stage, and HER2 expression, POM121 expression was also demonstrated as a relative factor for GC overall survival by multivariate Cox regression and Kaplan-Meier survival analyses. This evidence indicated that POM121 plays an important role in GC progression and invasion and has the potential to predict the prognosis of GC patients.

Soluble POM121, a variant that lacks the membrane-anchoring domain, was identified as a transcriptional regulator of gene promoters [24]. Kihlmark et al. reported POM121 may participate in the propagation of nuclear apoptosis [25]. The involvement of POM121 in transcriptional regulation and apoptosis suggests its potential role in tumorigenesis and progression. Rodriguez-Bravo et al. demonstrated the contribution of POM121 to tumorigenesis, cell proliferation, aggressiveness, and drug resistance in prostate cancer [15]. In lung cancer, decreased POM121 was confirmed to inhibit cell proliferation, clone formation, migration, and invasion [22]. We silenced and upregulated the POM121 expression in GC cells and detected the follow-up effects on cell biological functions. The results showed that downregulation of POM121 significantly hindered the proliferation, migration, and invasion of GC cells in vitro and vivo, while overexpression of POM121 expedited malignant biological properties in GC, suggesting the tumor-promoting role of POM121 in GC progression.

MYC, also named c-MYC, is an important proto-oncogene involved in cell regulation, proliferation, differentiation, and metabolism [26]. MYC is usually unexpressed in normal tissues, but can induce malignant transformation of normal cells when it is upregulated [27]. MYC is overexpressed in a variety of tumor tissues and shows significant influence on tumorigenesis and development [28, 29]. We constructed a PPI network around POM121, and found the underlying connection between POM121 and MYC. In addition, Pearson correlation indicated that POM121 was significant associated with MYC in GC tissues. We confirmed that silencing POM121 inhibited the expression of MYC via Western Blotting. PI3K/AKT signaling pathway plays a crucial role in the proliferation, apoptosis, angiopoiesis and metastasis of tumor [30-32]. MYC is also a downstream protein of PI3K/AKT pathway [33, 34]. We detected the expression and phosphorylation ofPI3K/AKT pathway after POM121 knockdown and overexpression, and found POM121 significantly promoted the phosphorylation level of the PI3K/AKT pathway. These results suggested that POM121 regulated MYC expression through PI3K/AKT pathway, thus affecting GC progression.

Conclusions

This study shows that POM121 is overexpressed in GC, and GC patients with high POM121 expression have a poor prognosis. POM121 promotes proliferation, clone formation, migration, and invasion of GC cells through

PI3K/AKT/MYC pathway. Therefore, POM121 might serve as a new prognostic factor and therapeutic target for GC patients.

Acknowledgements

We thank all patients enrolled in the study. We also thank H. Nikki March, PhD, from LiwenBianji, Edanz Editing China (www.liwenbianji.cn/ac), for editing the English text of a draft of this manuscript. This work was supported by grants from National Natural Science Foundation of China (82060438), Natural Science Foundation of Inner Mongolia Autonomous Region (2020MS08002, 2020MS08060, 2020MS08149, 2022MS08031), Inner Mongolia Autonomous Region Science and Technology Plan Project (2020GG0273, 2022YFSH0018), Bayannur city Science and Technology Plan Project (BYZ2019-1-2, K202025), Academician workstation (YSZ2018-2, 2020PT0010), Inner Mongolia Medical University Joint Project (YKD2021LH072), Inner Mongolia Autonomous Region Health Science and Technology Plan Project (202202402, 202201625, 202202405).

This study was performed in accordance with medical ethical standards and was approved by the Ethics Committee of Inner Mongolia Medical University. Written informed consents were obtained from all study participants. The animal study was reviewed and approved by the Ethics Committee of Inner Mongolia Medical University.

Disclosure of conflict of interest

None.

Address correspondence to: Lingli Zhang, Department of Ophthalmology, Inner Mongolia Autonomous Region People's Hospital, 42 Zhaowuda Road, Hohhot 010017, Inner Mongolia, China. E-mail: zlljlz9@163.com

References

[1] Xie J, Pang Y and Wu X. Taxifolin suppresses the malignant progression of gastric cancer by regulating the AhR/CYP1A1 signaling pathway. Int J Mol Med 2021; 48: 197.

[2] Chen W, Zheng R, Baade PD, Zhang S, Zeng H, Bray F, Jemal A, Yu XQ and He J. Cancer statistics in China, 2015. CA Cancer J Clin 2016; 66: 115-132.

[3] Raices M and D'Angelo MA. Nuclear pore complexes and regulation of gene expression. Curr Opin Cell Biol 2017; 46: 26-32.

[4] Pascualgarcia P and Capelson M. Nuclear pores as versatile platforms for gene regulation. Curr Opin Genet Dev 2014; 25: 110-117.

[5] Paul B and Montpetit B. Altered RNA processing and export leads to retention of mRNAs near transcription sites, nuclear pore complexes, or within the nucleolus. Mol Biol Cell 2016; 27: 2742-2756.

[6] Ren B, Cam H, Takahashi Y, Volkert T, Terragni J, Young RA and Dynlacht BD. E2F integrates cell cycle progression with DNA repair, replication, and G(2)/M checkpoints. Genes Dev 2002; 16: 245-256.

[7] Pascual-Garcia P, Debo B, Aleman JR, Talamas JA, Lan Y, Nguyen NH, Won KJ and Capelson M. Metazoan nuclear pores provide a scaffold for poised genes and mediate induced enhancer-promoter contacts. Mol Cell 2017; 66: 63-76.

[8] Kumar A, Sharma P, Gomar-Alba M, Shcheprova Z, Daulny A, Sanmartín T, Matucci I, Funaya C, Beato M and Mendoza M. Daughter-cell-specific modulation of nuclear pore complexes controls cell cycle entry during asymmetric division. Nat Cell Biol 2018; 7: 432-442.

[9] Lim KS and Wong RW. Targeting nucleoporin POM121-importin beta axis in prostate cancer. Cell Chem Biol 2018; 25: 1056-1058.

[10] Simon DN and Rout MP. Cancer and the nuclear pore complex. Adv Exp Med Biol 2014; 773: 285-307.

[11] Singer S, Zhao R, Barsotti AM, Ouwehand A, Fazollahi M, Coutavas E, Kai B, Neumann O, Longerich T, Pusterla T, Powers MA, Giles KM, Leedman PJ, Hess J, Grunwald D, Bussemaker HJ, Singer RH, Schirmacher P and Prives C. Nuclear pore component Nup98 is a potential tumor suppressor and regulates posttranscriptional expression of select p53 target genes. Mol Cell 2012; 48: 799-810.

[12] Rio-Machin A, Gómez-López G, Muñoz J, Garcia-Martinez F, Maiques-Diaz A, Alvarez S, Salgado RN, Shrestha M, Torres-Ruiz R, Haferlach C, Larráyoz MJ, Calasanz MJ, Fitzgibbon J and Cigudosa JC. The molecular pathogenesis of the NUP98-HOXA9 fusion protein in acute myeloid leukemia. Leukemia 2017; 31: 2000-2005.

[13] Xu H, Valerio DG, Eisold ME, Sinha A, Koche RP, Hu W, Chen CW, Chu SH, Brien GL, Park CY, Hsieh JJ, Ernst P and Armstrong SA. NUP98 fusion proteins interact with the NSL and MLL1 complexes to drive leukemogenesis. Cancer Cell 2016; 30: 863-878.

[14] Kin-Hoe C, Factor RE and Ullman KS. The nuclear envelope environment and its cancer connections. Nat Rev Cancer 2012; 12: 196-209.

[15] Rodriguez-Bravo V, Pippa R, Song WM, Carceles-Cordon M, Dominguez-Andres A, Fujiwara N, Woo J, Koh AP, Ertel A, Lokareddy RK,

Cuesta-Dominguez A, Kim RS, Rodriguez-Fernandez I, Li P, Gordon R, Hirschfield H, Prats JM, Reddy EP, Fatatis A, Petrylak DP, Gomella L, Kelly WK, Lowe SW, Knudsen KE, Galsky MD, Cingolani G, Lujambio A, Hoshida Y and Domingo-Domenech J. Nuclear pores promote lethal prostate cancer by increasing POM121-Driven E2F1, MYC, and AR nuclear import. Cell 2018; 174: 1200-1215, e20.

[16] Shaulov L, Gruber R, Cohen I and Harel A. A dominant-negative form of POM121 binds chromatin and disrupts the two separate modes of nuclear pore assembly. J Cell Sci 2011; 124: 3822-3834.

[17] Iwamoto M, Osakada H, Mori C, Fukuda Y, Nagao K, Obuse C, Hiraoka Y and Haraguchi T. Compositionally distinct nuclear pore complexes of functionally distinct dimorphic nuclei in the ciliate tetrahymena. J Cell Sci 2017; 130: 1822-1834.

[18] Yavuz S, Santarella-Mellwig R, Koch B, Jaedicke A, Mattaj IW and Antonin W. NLS-mediated NPC functions of the nucleoporin Pom121. FEBS Lett 2010; 584: 3292-3298.

[19] Zhao R, Tang G, Wang T, Zhang L, Wang W, Zhao Q and Zhao K. POM121 is a novel marker for predicting the prognosis of laryngeal cancer. Histol Histopathol 2020; 35: 1285-1293.

[20] Wang T, Sun H, Bao Y, En R, Tian Y, Zhao W and Jia L. POM121 overexpression is related to a poor prognosis in colorectal cancer. Expert Rev Mol Diagn 2020; 20: 345-353.

[21] Ma H, Li L, Jia L, Gong A, Wang A, Zhang L, Gu M and Tang G. POM121 is identified as a novel prognostic marker of oral squamous cell carcinoma. J Cancer 2019; 10: 4473-4480.

[22] Guan L, Zhang L, Wang T, Jia L, Zhang N, Yan H and Zhao K. POM121 promotes proliferation and metastasis in non-small-cell lung cancer through TGF-β/SMAD and PI3K/AKT pathways. Cancer Biomark 2021; 32: 293-302.

[23] Zhang S, Zheng C, Li D, Bei C, Zhang H, Tian R, Song X, Zhu X and Tan S. Clinical significance of POM121 expression in lung cancer. Genet Test Mol Biomarkers 2020; 24: 819-824.

[24] Franks TM, Benner C, Narvaiza I, Marchetto MC, Young JM, Malik HS, Gage FH and Hetzer MW. Evolution of a transcriptional regulator from a transmembrane nucleoporin. Genes Dev 2016; 30: 1155-1171.

[25] Kihlmark M, Imreh G and Hallberg E. Sequential degradation of proteins from the nuclear envelope during apoptosis. J Cell Sci 2001; 114: 3643-3653.

[26] Yoshida GJ. Emerging roles of Myc in stem cell biology and novel tumor therapies. J Exp Clin Cancer Res 2018; 37: 173.

[27] Liu Q, Sun Y, Fei Z, Yang Z, Duan K, Zi J, Cui Q, Yu M and Xiong W. Leptin promotes fatty acid oxidation and OXPHOS via the c-Myc/PGC-1 pathway in cancer cells. Acta Biochim Biophys Sin (Shanghai) 2019; 51: 707-714.

[28] Ireland AS, Micinski AM, Kastner DW, Guo B, Wait SJ, Spainhower KB, Conley CC, Chen OS, Guthrie MR, Soltero D, Qiao Y, Huang X, Tarapcsák S, Devarakonda S, Chalishazar MD, Gertz J, Moser JC, Marth G, Puri S, Witt BL, Spike BT and Oliver TG. MYC drives temporal evolution of small cell lung cancer subtypes by reprogramming neuroendocrine fate. Cancer Cell 2020; 38: 60-78.

[29] Feng YC, Liu XY, Teng L, Ji Q, Wu Y, Li JM, Gao W, Zhang YY, La T, Tabatabaee H, Yan XG, Jamaluddin MFB, Zhang D, Guo ST, Scott RJ, Liu T, Thorne RF, Zhang XD and Jin L. C-Myc inactivation of p53 through the pan-cancer lncRNA MILIP drives cancer pathogenesis. Nature Communications 2020; 11: 4980.

[30] Yang WB, Zhang WP, Shi JL and Wang JW. MiR-4299 suppresses non-small cell lung cancer cell proliferation, migration and invasion through modulating PTEN/AKT/PI3K pathway. Eur Rev Med Pharmacol Sci 2018; 22: 3408-3414.

[31] Karar J and Maity A. PI3K/AKT/mTOR pathway in angiogenesis. Front Mol Neurosci 2011; 4: 51.

[32] Feng FB and Qiu HY. Effects of artesunate on chondrocyte proliferation, apoptosis and autophagy through the PI3K/AKT/mTOR signaling pathway in rat models with rheumatoid arthritis. Biomed Pharmacother 2018; 102: 1209-1220.

[33] Zhang F, Li K, Yao X, Wang H, Li W, Wu J, Li M, Zhou R, Xu L and Zhao L. A miR-567-PIK3AP1-PI3K/AKT-c-Myc feedback loop regulates tumour growth and chemoresistance in gastric cancer-ScienceDirect. EBioMedicine 2019; 44: 311-321.

[34] Zhu F, Guo H, Bates PD, Zhang S, Zhang H, Nomie KJ, Li Y, Lu L, Seibold KR, Wang F, Rumball I, Cameron H, Hoang NM, Yang DT, Xu W, Zhang L, Wang M, Capitini CM and Rui L. PRMT5 is upregulated by B-cell receptor signaling and forms a positive-feedback loop with PI3K/AKT in lymphoma cells. Leukemia 2019; 33: 2898-2911.